

# Photodissociative spectroscopy of the hydroxymethyl radical (CH<sub>2</sub>OH) in the 3*s* and 3*p<sub>x</sub>* states

Lin Feng, Xin Huang, and Hanna Reisler

*Department of Chemistry, University of Southern California, Los Angeles, California 90089-0482*

(Received 9 May 2002; accepted 14 June 2002)

The absorption spectrum and photodissociation dynamics of the hydroxymethyl radical via its two lowest excited electronic states, 3*s* and 3*p<sub>x</sub>*, are investigated in a supersonic molecular beam by the depletion, resonance enhanced multiphoton ionization, and photofragment yield spectroscopy methods. The measured origins of the electronic transitions to the 3*s* and 3*p<sub>x</sub>* states agree with the most recent *ab initio* calculations. The vibronic bands of the  $2^2A'(3p_x) \leftarrow 1^2A''$  transition are much broader than those of the transition terminating in the  $2^2A''(3p_z)$  state, while the transition to the  $1^2A'(3s)$  state appears structureless. The investigation of the deuterated analog CH<sub>2</sub>OD shows that near the onset of the transition to the 3*s* state, only the O–D bond fission pathway is important, while both H and D products are detected following excitation to the 3*p<sub>x</sub>* state. The progressive broadening of the absorption features from the uppermost 3*p<sub>z</sub>* to the lowest 3*s* excited state is explained based on recent calculations of surface couplings to lower electronic states. These couplings also control the photodissociation dynamics and the reaction outcomes. © 2002 American Institute of Physics. [DOI: 10.1063/1.1498469]

## I. INTRODUCTION

The hydroxymethyl radical (CH<sub>2</sub>OH) has attracted considerable attention in recent years. It is a significant product in the reaction of O(<sup>1</sup>D) with methane and ethane,<sup>1,2</sup> and reactions of Cl atoms and OH radicals with methanol also yield predominantly CH<sub>2</sub>OH.<sup>3–5</sup> Owing to the low and comparable barriers to isomerization and dissociation, the isomerization CH<sub>2</sub>OH ↔ CH<sub>3</sub>O has commanded much theoretical interest.<sup>6–10</sup> According to *ab initio* calculations,<sup>11</sup> the lowest excited electronic states of CH<sub>2</sub>OH have a predominant Rydberg character; specifically, the 3*s*, 3*p<sub>x</sub>*, 3*p<sub>y</sub>*, and 3*p<sub>z</sub>* states. Of these four states, only the 3*p<sub>y</sub>* state does not carry oscillator strength, while the transitions to 3*p<sub>x</sub>* and 3*p<sub>z</sub>* are the strongest. The ground state of the hydroxymethyl radical is described by the configuration,

$$\cdots(\sigma_{co})^2(\pi_{co})^2(n_o)^2(\pi_{co}^*)^1.$$

The Rydberg states are obtained by promoting the electron in the half-occupied  $\pi_{co}^*$  antibonding molecular orbital to a Rydberg orbital localized on the carbon atom. Johnson and Hudgens carried out *ab initio* calculations of the neutral radical and its cation.<sup>4</sup> Their results show that the ground state of the CH<sub>2</sub>OH radical is nonplanar, belonging to the *C*<sub>1</sub> symmetry point group. However, because of the shallowness of the CH<sub>2</sub> wag angular potential, the electronic wave function complies with *C<sub>s</sub>* *A''* symmetry when taking into consideration the rapid interconversion of the mirror structures. The Rydberg states have a planar geometry, similar to that of the bound CH<sub>2</sub>OH<sup>+</sup> cation.<sup>4</sup> Therefore, the 3*s* and 3*p<sub>x</sub>* states are denoted in this paper by  $2^2A'(3p_x)$  and  $1^2A'(3s)$ , and the electronic transitions are labeled by *C<sub>s</sub>* symmetry.

The assignments of the transitions to these Rydberg states have been the subject of some controversy.<sup>11–15</sup> The experimentally observed absorption band at 41 062 cm<sup>-1</sup>

was initially assigned as the origin band of the  $2^2A'(3p_x) \leftarrow 1^2A''$  system.<sup>4,11</sup> Aristov *et al.* revised this assignment to  $2^2A''(3p_z) \leftarrow 1^2A''$ , based on spectroscopic simulations of rotational contours for selected vibronic bands obtained by resonance enhanced multiphoton ionization (REMPI) in the molecular beam and in a flow cell.<sup>12</sup> *Ab initio* calculations carried out by Bruna and Grein supported this revision,<sup>13</sup> but a later computation by Chen and Davidson favored the initial assignment of the upper state as 3*p<sub>x</sub>*.<sup>14</sup> Later on, Bruna and Grein recalculated the adiabatic and vertical transition energies to the four Rydberg states,<sup>15</sup> which reconfirmed their original assignments, and resulted in a much lower energy for the 3*s* state than in the previous theoretical works.<sup>11</sup>

In our previous publications, the molecular beam spectroscopy and photodissociation dynamics of the hydroxymethyl radical in the origin band of the 3*p<sub>z</sub>* Rydberg state were reported.<sup>12,16,17</sup> We estimated the lifetime of the 3*p<sub>z</sub>* state at 0.5 ± 0.1 ps, and established that H+CH<sub>2</sub>O(1<sup>1</sup>A<sub>1</sub>) was a major dissociation channel following origin band excitation. The two lowest excited states, 3*s* and 3*p<sub>x</sub>*, have never been identified in molecular beam spectroscopy. Their origins were tentatively assigned based on the UV absorption spectrum obtained at 298 K,<sup>3</sup> the same spectrum for which the bands assigned to the 3*p<sub>x</sub>* state were later reassigned to 3*p<sub>z</sub>*.<sup>12</sup> Knowledge of the spectroscopy and the photophysics related to these two lowest states should provide valuable insights into the UV photodissociation dynamics of the radical.

In this paper, we report the first spectroscopic study of the UV excitation of CH<sub>2</sub>OH and CH<sub>2</sub>OD to the 3*s* and 3*p<sub>x</sub>* states in the molecular beam. We assign the origins of the electronic transitions to these two states, estimate their lifetimes, and identify the channels responsible for H/D products. The experimentally determined band origins are in ex-

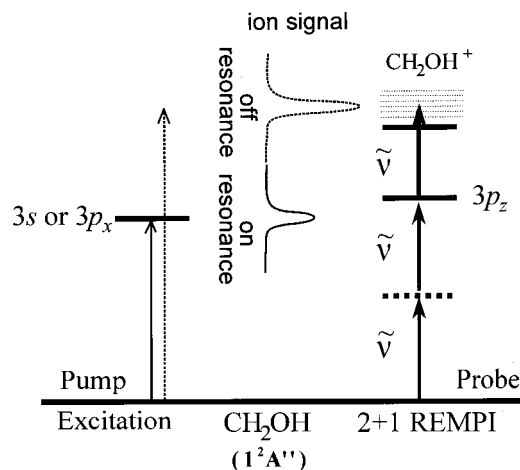
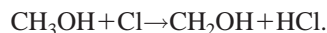
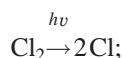


FIG. 1. Schematic representation of the depletion method. When the pump frequency matches an absorption band in the transition to the  $3s$  or  $3p_x$  states, the population of the ground state is reduced. Consequently, the 2+1 REMPI probe signal ( $\text{CH}_2\text{OH}^+$ ) centered on the origin band of the  $2^2A''(3p_z) \leftarrow 1^2A''$  transition is depleted compared to the off-resonance signal.

cellent agreement with the recent *ab initio* calculations of Bruna and Grein.<sup>13,15</sup> With the aid of the calculations performed by Hoffman and Yarkony (HY) on conical intersections between the ground and low-lying Rydberg states of  $\text{CH}_2\text{OH}$ ,<sup>18</sup> we are also able to identify the pathways that lead from the initially excited electronic states to H(D) products of  $\text{CH}_2\text{OD}$ .

## II. EXPERIMENT

The experimental arrangement and procedures have been reported elsewhere,<sup>12,16</sup> and only aspects specific to this study are described in detail. Reactant mixtures of  $\text{Cl}_2$ ,  $\text{CH}_3\text{OH}$ , or  $\text{CH}_3\text{OD}$  (Aldrich, used without further purification), and He are prepared in a glass bulb at 300 K and transported into the vacuum chamber through a piezoelectrically controlled pulsed nozzle. The hydroxymethyl radical is produced at the end of a quartz-nozzle attachment by the reactions:



Photodissociation of  $\text{Cl}_2$  is accomplished by pulsed 355 nm radiation from a Nd:YAG laser (Spectra Physics, GCR-11; 8 mJ, focused by a 30 cm f.l. cylindrical lens). By controlling the position of the laser beam along the quartz tube, the rapid consecutive reaction  $\text{Cl} + \text{CH}_2\text{OH} \rightarrow \text{CH}_2\text{O} + \text{HCl}$  can be suppressed. Hydroxymethyl radicals with densities of  $10^{12}$ – $10^{13}$   $\text{cm}^{-3}$  are produced with a rotational temperature of about 10 K. No vibrational “hot bands” are observed.

Three types of spectra are recorded: (a) depletion spectra, (b) H and D photofragment yield spectra of  $\text{CH}_2\text{OD}$ , (c) 2+2 REMPI spectra. Two-laser experiments are carried out with the laser beams counterpropagating, and crossing the molecular beam at the center of the reaction chamber at  $90^\circ$ . In the depletion method, shown schematically in Fig. 1, the

UV pump radiation from a Nd:YAG laser-pumped OPO (Continuum, PL8000/Sunlite FX-1; 0.5 mJ; 40 cm f.l. lens) accesses either the  $3p_x$  or the  $3s$  state by one-photon excitation. A Nd:YAG laser pumped dye laser (Continuum, PL8010/ND6000, Coumarin 480; 2 mJ, 15 cm f.l. lens) serves as the probe laser whose frequency is fixed at 487.07 nm ( $20\,531\text{ cm}^{-1}$ ) to access (by 2+1 REMPI) the peak of the  $2^2A''(3p_z) \leftarrow 1^2A''$  origin band of  $\text{CH}_2\text{OH}$ .<sup>12,16</sup> The pump laser is scanned from 26 000 to 42 000  $\text{cm}^{-1}$ , covering the range of the anticipated transitions to the  $3p_x$  and  $3s$  states. The population of the ground state is depleted whenever photon absorption to an excited state takes place thereby attenuating the  $\text{CH}_2\text{OH}^+$  ion signal. The relative absorption to the  $3s$  or  $3p_x$  state is calculated as the percent reduction in the  $\text{CH}_2\text{OH}^+$  ion signal:

$$P_{\text{absorption}}(3s \text{ or } 3p_x) = \frac{I_{\text{pump off}} - I_{\text{pump on}}}{I_{\text{pump off}}} \times 100\%. \quad (1)$$

The signal intensities,  $I$ , on the right-hand side of Eq. (1) are obtained by using gated integrators to average the  $\text{CH}_2\text{OH}^+$  ion signal for several laser shots. “Pump off” and “pump on” conditions are accomplished by reversing the order of firings of the pump and probe lasers. The time delay is regulated by digital pulse/delay generators (DG 535, Stanford Research Systems, 10 ns resolution). In the case of “pump off,” the probe laser precedes the pump laser by 100 ns, while with “pump-on,” the probe laser is fired 20 ns after the pump. The observed signals are normalized to suppress the probe power fluctuations. The pump laser power is optimized to achieve a good signal-to-noise ratio, while maintaining a linear dependence of the depletion signal on intensity. Each data point reflects the average of 20 measurements.

H and D photofragments from  $\text{CH}_2\text{OD}$  are detected by 1+1' two-color REMPI via the  $L\text{-}\alpha$  transition at 121.6 nm. The doubled output ( $\sim 365$  nm, 3 mJ) of a Nd:YAG laser pumped dye laser system (Continuum, PL8010/ND6000, LDS 751) is focused into a mixture of Kr:Ar (120:490 Torr) in a tripling cell. A  $\text{MgF}_2$  lens (75 mm f.l.) then refocuses the tripled 121.6 nm radiation into the chamber.

In the one-color 2+2 REMPI method, the laser radiation (560–580 nm, 8 mJ) is focused by a 15 cm f.l. lens. Simultaneous absorption of two photons excites the radical resonantly to the  $3p_x$  Rydberg state, while additional two photons of the same wavelength are required to ionize the excited molecules.

In all three methods, the generated ions are accelerated toward a 25 mm diameter multi-channel plate (MCP) detector (Galileo, 25 mm) through a vertically mounted Wiley–McLaren time-of-flight (TOF) mass spectrometer. The MCP output is amplified by a wide-band amplifier (KOTA microcircuits, KE104), and the signal is digitized by a 500 MHz oscilloscope (Tektronix, TDS640A controlled with LabView programs). Typically, 20–50 laser firings are averaged.

## III. RESULTS AND DISCUSSIONS

### A. Excitation to the $3p_x$ state of $\text{CH}_2\text{OH(D)}$

In the depletion spectrum shown in Fig. 2, the pump frequency is scanned over the range 32 000–42 000  $\text{cm}^{-1}$ ,

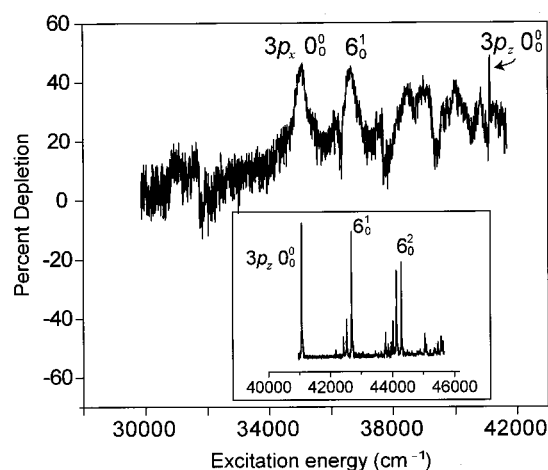


FIG. 2. Depletion spectrum of  $\text{CH}_2\text{OH}$ . The sharp peak at  $41\,062\text{ cm}^{-1}$  is the origin band of the  $2^2A''(3p_z)\leftarrow 1^2A''$  transition. The peaks at  $35\,063$  and  $36\,670\text{ cm}^{-1}$  correspond to the origin band and the C–O stretch ( $6_0^1$ ) of the  $2^2A'(3p_x)\leftarrow 1^2A''$  transition. For comparison, the REMPI spectrum of the  $2^2A''(3p_z)\leftarrow 1^2A''$  transition is reproduced in the inset at the bottom (Ref. 12).

with the probe laser frequency fixed at  $20\,531\text{ cm}^{-1}$ , i.e., half the frequency necessary to reach the band origin of the  $2^2A''(3p_z)\leftarrow 1^2A''$  transition. The first observed vibronic band, at  $35\,063\text{ cm}^{-1}$ , is assigned as the origin of the  $2^2A'(3p_x)\leftarrow 1^2A''$  transition. This assignment is based on the most recent theoretical calculations,<sup>13,15</sup> and the fact that it is the first in a series of distinct bands. The second peak, which is  $1607\text{ cm}^{-1}$  higher in energy than the first, is assigned as the C–O stretch,  $6_0^1$ . This transition frequency is consistent with the C–O stretch vibrational frequency of  $1643\text{ cm}^{-1}$  calculated *ab initio* for the ground state  $\text{CH}_2\text{OH}^+$  ion.<sup>4</sup> The origin band of the  $2^2A''(3p_z)\leftarrow 1^2A''$  system is also observed in the depletion spectrum using the same detection scheme, as the much narrower spectral feature at  $\sim 41\,000\text{ cm}^{-1}$ . Note that the  $2^2A'(3p_x)\leftarrow 1^2A''$  system is a perpendicular (out-of-plane) transition, while the transition moment of the  $2^2A''(3p_z)\leftarrow 1^2A''$  system is parallel to the CO bond.<sup>11,13,15</sup> This can cause detection difficulties in depletion experiments when excitation and detection are accomplished via one-photon transitions. However, the problem is circumvented in our experiments in which the 2+1 REMPI excitation scheme is exploited for the probe transition. In this protocol, the two upper states are monitored with comparable efficiencies. For comparison, displayed as the inset in Fig. 2 is a portion of the assigned 2+1 REMPI spectrum of  $\text{CH}_2\text{OH}$  in the region  $41\,000\text{--}45\,000\text{ cm}^{-1}$ , which shows the vibronic bands belonging to the  $2^2A''(3p_z)\leftarrow 1^2A''$  system.<sup>12</sup> This spectrum exhibits a progression in the C–O stretch, reflecting the large C–O bond length difference between the ground and the upper states.<sup>4,12</sup> The vibrational progressions in the two transitions terminating in the  $3p_x$  and  $3p_z$  states are expected to be quite similar, as indeed observed, because both involve excitation to Rydberg states that converge to the ground state of the core ion,  $\text{CH}_2\text{OH}^+$ .

To date, the only available spectral information for this energy region has been the absorption spectrum measured

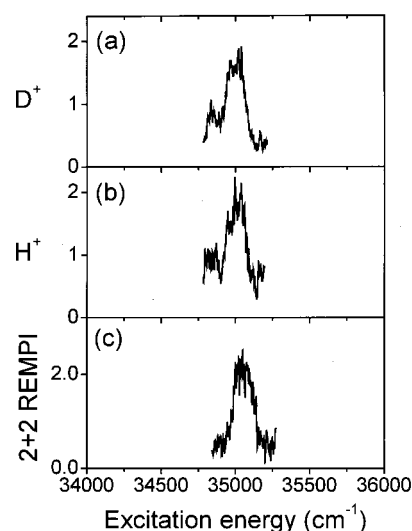


FIG. 3. Photofragment yield and 2+2 REMPI spectra of  $\text{CH}_2\text{OD}$ . In (a) and (b) signals from D and H products from  $\text{CH}_2\text{OD}$  are recorded for the  $2^2A'(3p_x)\leftarrow 1^2A''$  origin band. In (c) the 2+2 REMPI spectrum of  $\text{CH}_2\text{OD}$  in the same region is shown.

at  $298\text{ K}$ , where all the vibrational bands exhibit similar widths.<sup>3</sup> In the supersonic beam the spectral broadening due to rotational structure is effectively eliminated, and it becomes obvious that the vibronic bands of the  $2^2A'(3p_x)\leftarrow 1^2A''$  transition are much broader than those of the corresponding transition to the  $3p_z$  state. Also, in both the depletion and the UV absorption spectra, an underlying continuum is apparent. The spectral simulations of Aristov *et al.* confirm that the breadths of the vibronic bands are proportional to their lifetimes.<sup>12</sup> The broad peaks in the  $2^2A'(3p_x)\leftarrow 1^2A''$  system indicate that the  $3p_x$  state is predissociating rapidly, with a lifetime much shorter than that of the  $2^2A''(3p_z)$  state. Since both states are predissociative, the observed depletion fractions can be high (Fig. 2), approaching 50%.

In order to identify the dissociation pathways, we measured photofragment yield spectra of the isotopic analog  $\text{CH}_2\text{OD}$ , and detected both H and D fragments. The band shapes and widths of the D and H photofragments measured in the region of the origin band and shown in Figs. 3(a) and 3(b) match those observed in the 2+2 REMPI spectrum of  $\text{CH}_2\text{OD}$  [Fig. 3(c)], and in the depletion spectrum of  $\text{CH}_2\text{OH}$  (Fig. 2). The coincident appearance of these peaks confirms that the  $3p_x$  Rydberg state is the source of both H and D products from  $\text{CH}_2\text{OD}$ .

## B. The $3s$ state of $\text{CH}_2\text{OH(D)}$

Since the  $3s$  state is the lowest excited state of  $\text{CH}_2\text{OH}$ , the interpretation of its photodissociation dynamics should be simplified, as it would involve fewer possible electronic states. We searched for the origin of the transition to the  $3s$  state near the energy predicted by the *ab initio* calculations; i.e.,  $3.31\text{ eV}$ .<sup>15</sup> We were unable to observe a REMPI spectrum in this region, but using the depletion method, we detected a broad absorption feature starting at  $26\,000\text{ cm}^{-1}$  ( $3.21\text{ eV}$ ) [Fig. 4(a)]. The absorption does not cease above  $28\,500\text{ cm}^{-1}$ , but extends to shorter wavelengths, and con-

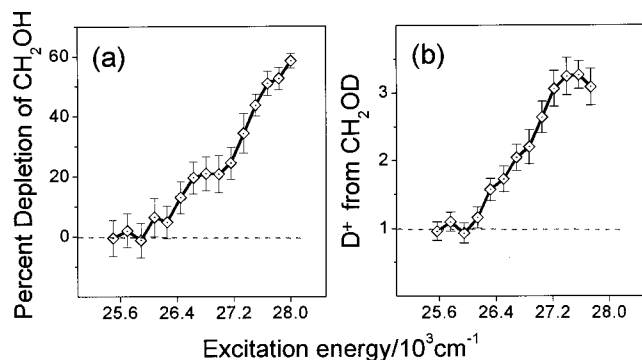


FIG. 4. (a) Depletion spectrum of CH<sub>2</sub>OH at the onset of the  $1^2A'(3s) \leftarrow 1^2A''$  transition. (b) The corresponding D photofragment yield spectrum of CH<sub>2</sub>OD.

stitutes the underlying continuum near the band origins of the transitions to the  $3p_x$  and  $3p_z$  states, as described above. The dissociative nature of the  $3s$  state explains the absence of a REMPI spectrum in this region. Our assignment of the depletion spectrum to the  $1^2A'(3s) \leftarrow 1^2A''$  transition is based on the proximity of its onset to the theoretical prediction,<sup>13,15</sup> and the absence of any detectable absorptions at lower excitation energies. This band edge is also confirmed in the D photofragment yield spectrum of CH<sub>2</sub>OD [Fig. 4(b)]. Similar to the depletion spectrum of CH<sub>2</sub>OH, the D photofragment yield spectrum of CH<sub>2</sub>OD also appears structureless. In contrast to the excitation in the region of the  $3p_x$  origin band, we could not detect H products in this region within our sensitivity. This is the first time that absorption in this region is recorded.

### C. Spectroscopy and photochemistry

Table I summarizes the energy positions of the  $3s$ ,  $3p_x$ , and  $3p_z$  states of CH<sub>2</sub>OH determined experimentally in our work, and compares them with the most recent theoretical results. Our results agree very well with the calculation of Bruna and Grein,<sup>13,15</sup> but not with that of Chen and Davidson.<sup>14</sup> Although both calculations use similar *ab initio* methods, Bruna and Grein explain that Chen and Davidson overestimate the energies of the upper states, because they use directly diagonalized energy eigenvalues in their MRCI calculations, which are higher than those obtained using the extrapolated or estimated full CI results by 0.5–0.8 eV.<sup>15</sup>

Considering the fact that the  $3s$ ,  $3p_x$ , and  $3p_z$  states are predominantly Rydberg in character with identical ionic

TABLE I. Theoretically calculated and experimentally determined origin bands for the transitions terminating in the  $3s$  and  $3p_x$  states of CH<sub>2</sub>OH.

State	$T_0^E$ (eV) Theory <sup>a</sup>	$T_0^E$ (eV) Theory <sup>b</sup>	$T_0$ (eV) Expt. <sup>c</sup>
$3s$	4.12	3.31	3.22
$3p_x$	5.20	4.41	4.34
$3p_z$	5.80	5.06	5.09 <sup>d</sup>

<sup>a</sup>Reference 14.

<sup>b</sup>Reference 15; calculated at the geometry of CH<sub>2</sub>OH<sup>+</sup>.

<sup>c</sup>This work.

<sup>d</sup>References 12 and 16.

cores (the ground state of CH<sub>2</sub>OH<sup>+</sup>), our observation of a featureless transition to the  $3s$  state is intriguing. It is noteworthy that a similar behavior has been observed in other hydrocarbon radicals, such as CH<sub>3</sub> and C<sub>2</sub>H<sub>5</sub>.<sup>19–21</sup> C<sub>2</sub>H<sub>5</sub> in particular provides a good analog to the isoelectronic CH<sub>2</sub>OH. Its UV absorption spectrum in the region of excitation to the  $3s$  Rydberg state (230–265 nm) is also broad and structureless, while absorption to the  $3p$  states exhibit characteristic vibronic structure.<sup>20</sup> There is no apparent local minimum on the  $3s$  state of C<sub>2</sub>H<sub>5</sub>, and the absence of structural features in the spectrum was interpreted based on fast dissociation via both internal conversion to a low-lying surface, and prompt dissociation on the excited state proceeding via a  $C_{2v}$  pathway.<sup>21</sup> There are, undoubtedly, many differences between C<sub>2</sub>H<sub>5</sub> and CH<sub>2</sub>OH, but nevertheless some similarities in the Rydberg–valence and Rydberg–continuum interactions of these two radicals are expected.

The conical intersection calculations of HY pinpoint pathways for radiationless decay, which are expected to play an essential role in the photodissociation dynamics on the  $3s$  and  $3p_x$  states.<sup>18</sup> An efficient seam of conical intersections between  $3s$  and the ground state has been revealed in these calculations. A low-energy crossing seam was found at 2.9 eV, at an O–H distance of about 1.48 Å, which is extended by about 0.5 Å from the equilibrium O–H distance in the ground state. The vertical cone greatly promotes radiationless transitions from  $3s$  to the ground state. After the  $3s$ /ground state coupling, CH<sub>2</sub>OH(D) dissociates directly to H<sub>2</sub>CO( $1^1A_1$ ) + H(D), as a result of the low dissociation energy for this channel (~1.3 eV), and the large value of R(O–H) accessed on the ground state. Our observation of abundant D production in CH<sub>2</sub>OD excited near the onset of the transition to the  $3s$  state is consistent with this mechanism. The conical intersection energy is about 1.2 eV lower than the vertical energy of excitation to the  $3s$  state, which is ~4.1 eV in HY's calculation. No local energy minimum is found along this route, and HY predict that the  $3s$  state would be structureless, as confirmed in our experiments.

In the absorption and depletion spectra in the energy range 30 000–40 000 cm<sup>-1</sup>, the distinct vibronic transitions to the  $3p_x$  state are superimposed on a weak continuum, which is attributed to the structureless absorption to the  $3s$  state. Because the  $3s$  state is essentially repulsive with a calculated vertical transition energy of about 4.1 eV (~33 000 cm<sup>-1</sup>), the extension of the  $1^2A'(3s) \leftarrow 1^2A''$  absorption to energies up to about 40 000 cm<sup>-1</sup> is reasonable.

The photochemistry following  $3p_x$  excitation is more complicated due to the multiple couplings and pathways involved in the photodissociation. This state is bound but predissociative, as indicated by its broadened vibrational bands. According to the calculations,<sup>18</sup> after the radical reaches the  $3p_x$  state, it first couples to the  $3s$  state, and subsequently to the ground state as described above. Because of the proximity of the  $3p_x$  to the  $3s$  state, Franck–Condon considerations would favor initial coupling between these two states.

The conical intersection between  $3p_x$  and  $3s$  is located at 4.7 eV with one of the C–H bonds elongated by 0.3 Å

with respect to the equilibrium bond length in the ground state. On the  $3s$  state, the crossing occurs at  $O-H=0.98 \text{ \AA}$  and  $C-H=1.40 \text{ \AA}$ , leading to two subsequent intersections between  $3s$  and the ground state. The one at 4.5 eV terminates at a large  $C-H$  bond distance on the ground state, and the other occurs at an extended  $O-H$  bond length. These crossing seams provide readily accessible routes to  $HCOH(HCOD)+H$  and  $H_2CO+H(D)$ , respectively. The appearance of both H and D products in the  $CH_2OD$  photofragment yield spectrum can be explained by this crossing mechanism.

The theoretically estimated  $C-H$  bond dissociation energy in  $CH_2OH$  is 3.91 eV,<sup>18</sup> while the  $3s$ /ground state calculated intersection energy at large  $C-H$  bond distance is 4.5 eV. These energies are higher than those of the observed onset of the transitions to the  $3s$  state (3.22 eV), which explains the absence of H products when  $CH_2OD$  is excited near the threshold of the  $1^2A'(3s) \leftarrow 1^2A''$  absorption. Apparently, isomerization to the methoxy radical does not take place at these excitation energies. Results of kinetic energy release experiments in the H and D channels and H/D ratio measurements support this interpretation, but are beyond the scope of this paper, and will be reported separately.

#### IV. SUMMARY

By combining depletion, REMPI and photofragment yield spectroscopy studies of the  $CH_2OH(D)$  radical in the molecular beam, we have identified the electronic transitions to the two lowest excited states,  $3s$  and  $3p_x$ . The measured transition energies agree well with the *ab initio* calculations of Bruna and Grein.<sup>13,15</sup> The photofragment yield spectra for H and D from  $CH_2OD$  can be understood in terms of the conical intersections between the two excited states and between  $3s$  and the ground state as calculated by Hoffman and Yarkony. D production following excitation to the  $3s$  state involves an efficient conical intersection with the ground state. Dissociation via the  $3p_x$  state is indirect, and involves multiple surface crossings terminating in  $O-H$  and  $C-H$  bond fission on the ground electronic surface.<sup>18</sup> No evidence for isomerization to the methoxy radical is obtained.

#### ACKNOWLEDGMENTS

Support from the Chemical Sciences, Geosciences and Biosciences Division, Office of Basic Energy Sciences, U.S. Department of Energy, and the Donors of the Petroleum Research Fund, administered by the American Chemical Society are gratefully acknowledged. Part of the equipment used in this experiment was purchased with NSF support. We are indebted to David Yarkony for discussions regarding conical intersections in  $CH_2OH$ , and to F. Grein and D. Yarkony for sending results prior to publication. We thank Dr. Oleg Boyarkin for his contributions in the initial stages of this work.

- <sup>1</sup>J. J. Lin, J. Shu, Y. T. Lee, and X. Yang, *J. Chem. Phys.* **113**, 5287 (2000).
- <sup>2</sup>J. Shu, J. J. Lin, Y. T. Lee, and X. Yang, *J. Chem. Phys.* **115**, 849 (2001).
- <sup>3</sup>P. Pagsberg, J. Munk, A. Sillesen, and C. Anastasi, *Chem. Phys. Lett.* **146**, 375 (1988).
- <sup>4</sup>R. D. Johnson and J. W. Hudgens, *J. Phys. Chem.* **100**, 19874 (1996), and references therein.
- <sup>5</sup>M. Ahmed, D. S. Peterka, and A. G. Suits, *Phys. Chem. Chem. Phys.* **2**, 861 (2000).
- <sup>6</sup>G. F. Adams, R. J. Bartlett, and G. D. Purvis, *Chem. Phys. Lett.* **87**, 311 (1982).
- <sup>7</sup>S. Saebø, L. Radom, and H. F. Schaefer III, *J. Chem. Phys.* **78**, 845 (1983).
- <sup>8</sup>S. P. Walch, *J. Chem. Phys.* **98**, 3076 (1993).
- <sup>9</sup>C. W. Bauschlicher and H. Partridge, *J. Phys. Chem.* **98**, 1826 (1994).
- <sup>10</sup>C. Oehlers, H. G. Wagner, H. Ziemer, F. Temps, and S. Dobe, *J. Phys. Chem. A* **104**, 10500 (2000).
- <sup>11</sup>S. Rettrup, P. Pagsberg, and C. Anastasi, *Chem. Phys.* **122**, 45 (1988).
- <sup>12</sup>V. Aristov, D. Conroy, and H. Reisler, *Chem. Phys. Lett.* **318**, 393 (2000).
- <sup>13</sup>P. J. Bruna and F. Grein, *J. Phys. Chem. A* **102**, 3141 (1998).
- <sup>14</sup>F. Chen and E. R. Davidson, *J. Phys. Chem. A* **105**, 4558 (2001).
- <sup>15</sup>P. J. Bruna and F. Grein, *J. Phys. Chem. A* **105**, 8599 (2001).
- <sup>16</sup>D. Conroy, A. Aristov, L. Feng, and H. Reisler, *J. Phys. Chem. A* **104**, 10288 (2000).
- <sup>17</sup>D. Conroy, A. Aristov, L. Feng, A. Sanov, and H. Reisler, *Acc. Chem. Res.* **34**, 625 (2001).
- <sup>18</sup>B. C. Hoffman and D. R. Yarkony, *J. Chem. Phys.* **116**, 8300 (2002).
- <sup>19</sup>S. W. North, D. A. Blank, P. M. Chu, and Y. T. Lee, *J. Chem. Phys.* **102**, 792 (1995).
- <sup>20</sup>J. Munk, P. Pagsberg, E. Ratajczak, and A. Sillesen, *J. Phys. Chem.* **90**, 2752 (1986).
- <sup>21</sup>G. Amaral, K. Xu, and J. Zhang, *J. Chem. Phys.* **114**, 5164 (2001).